International Journal of General Medicine

Dovepress
open access to scientific and medical research

Open Access Full Text Article

ORIGINAL RESEARCH

Identification of *PDZD11* as a Potential Biomarker Associated with Immune Infiltration for Diagnosis and Prognosis in Epithelial Ovarian Cancer

Xiaoqi Chen[1,2,*], Zhuang Li[1,*], Yanying Feng[3], Zhijun Yang[1,2], Bingbing Zhao[1,2]

[1]Department of Gynecologic Oncology, Guangxi Medical University Cancer Hospital, Nanning, Guangxi, 530021, People's Republic of China; [2]Key Laboratory of Early Prevention and Treatment for Regional High Frequency Tumor (Guangxi Medical University), Ministry of Education, Nanning, Guangxi, 530021, People's Republic of China; [3]Department of Cardiopulmonary Center, Guangxi Medical University Cancer Hospital, Nanning, Guangxi, 530021, People's Republic of China

*These authors contributed equally to this work

Correspondence: Bingbing Zhao; Zhijun Yang, Department of Gynecologic Oncology, Guangxi Medical University Cancer Hospital, No. 71 Hedi Road, Nanning, Guangxi, 530021, People's Republic of China, Email zhaobingbing@gxmu.edu.cn; yzj7528@126.com

Purpose: Evidence has indicated that *PDZD11* is involved in regulating adherens junction. However, the distinct effect of its aberrant expression on epithelial ovarian cancer (EOC) awaits clarification.

Methods: In this study, public databases (Gene Expression Omnibus, The Cancer Genome Atlas, and The Genotype-Tissue Expression), online analysis tools (Kaplan-Meier plotter and TIMER), and data analysis methods (Gene Ontology, Kyoto Encyclopedia of Genes and Genomes, and the CIBERSORT algorithm) were fully utilized to analyze the differential expression, diagnostic efficiency, prognostic significance, potential function, and correlation with immune infiltration of PDZD11. The differential expression of *PDZD11* was tested by immunohistochemistry in EOC tissues (78 cases) and control tissues (37 cases).

Results: Our results indicate that *PDZD11* was remarkably overexpressed in EOC, which was associated with advanced cancer stages, no lymphatic metastasis status, and poor prognosis. Moreover, *PDZD11* played a role in cell adhesion, cell proliferation, and immune responses. Also, *PDZD11* was significantly related to the abundances of infiltrating immune cells in EOC, including neutrophils, macrophages, dendritic cells, CD8+ T cells, and CD4+ T cells, and its expression was positively co-expressed with well-known immune checkpoints, including TIGIT, TIM3, LAG3, CTLA4, and PD-1.

Conclusion: These results suggest that *PDZD11* could be a potential diagnostic and prognostic biomarker associated with immune infiltration in EOC, and our findings might help elucidate the function of *PDZD11* in carcinogenesis.

Keywords: *PDZD11*, epithelial ovarian cancer, prognostic biomarker, immune infiltration, immune checkpoint

Introduction

Epithelial ovarian cancer (EOC) is ranked as one of the most lethal gynecological cancers. Type II EOCs, including high-grade serous ovarian cancer, have a particularly poor prognosis because they are characterized by high-frequency oncogene mutations, including *P53* and *BRCA*, and are more likely to invade and spread.[1] In 2020, 313,959 women were diagnosed with EOC worldwide, and 207,252 women died from it; the incidence and age-world-standardized mortality rate of this disease is 6.6 and 4.2 per 100,000, respectively.[2] The tumor spreads easily to the pelvic and abdominal cavities and about 75% of cases are diagnosed at an advanced stage.[3]*BRCA1* and *BRCA2* mutations carriers account for about 6–15% of EOC cases, and these cases present a better response to platinum-based chemotherapy and poly ADP-ribose polymerase (PARP) inhibitors, which has improved the survival rate of EOC patients to some extent.[4] However, the overall treatment of advanced EOC remains challenging. Frustratingly, early detection is difficult for EOC due to its asymptomatic nature in the early stages. Although the number of asymptomatic ovarian masses found in late

Received: 13 January 2024
Accepted: 22 April 2024
Published: 14 May 2024

Graphical Abstract

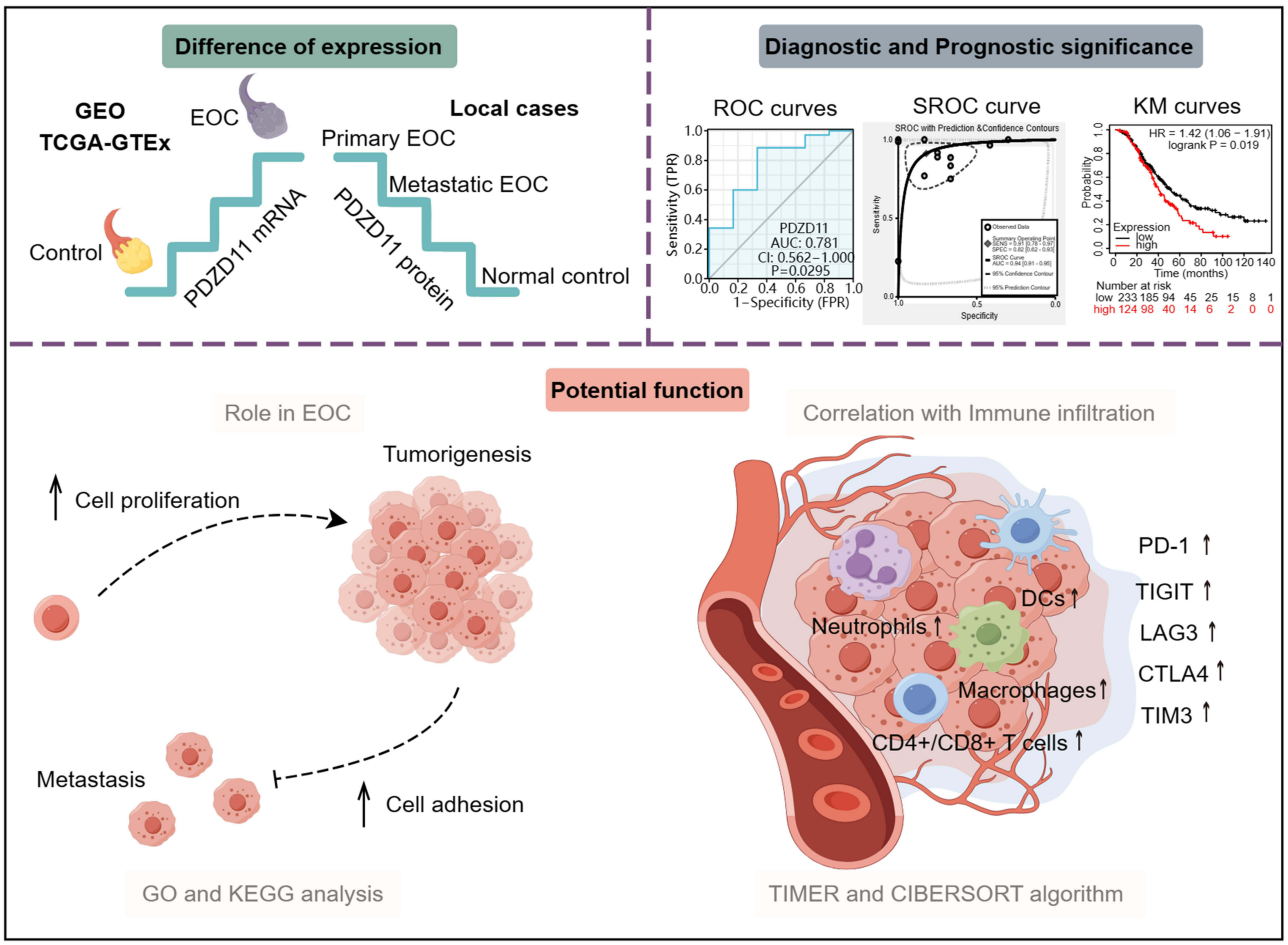

childbearing women has increased with the use of prenatal ultrasound,[5] early EOC detection rate has not been greatly improved. At present, CA125 and HE4 are the only approved biomarkers for EOC. Some evidence suggests that various biomarkers combined with patient characteristics into a multivariate index, such as OVA1, ROMA, and Overa, could increase the detection rate of early EOC.[6] However, they are not sufficient for EOC early diagnosis. Searching for effective biomarkers to detect and diagnose this cancer and to predict the outcomes of patients has thus become imperative.

PDZ Domain Containing 11 (*PDZD11*), a small protein widely expressed in the body, is mainly comprised of a single PDZ domain.[7] *PDZD11* has often been reported to be associated with the adherens junction (AJ) of epithelial cells.[8–11] AJ is a component of cell–cell junctions and is essential for maintaining cell–cell adhesion. *PDZD11* binds nectins to the cadherin-and cytoskeleton-related protein complex by interacting with PLEKHA7 to stabilize the nexins at AJs and promotes efficient early assembly of junctions.[9] Some aberrantly expressed AJ-related molecules have been shown to be potential prognostic biomarkers or therapeutic targets for certain cancers.[12,13] Regrettably, the role of *PDZD11* as a cell adhesion-related protein in tumors has rarely been studied. The aim of this study was to provide new insights into the underlying regulatory effects of *PDZD11* on carcinogenesis and immune infiltration as well as its application as a diagnostic and prognostic biomarker for EOC.

Methods

Data Mining and Processing

The mRNA expression data (Table S1) in this study were accessed from Gene Expression Omnibus (GEO),[14] The Cancer Genome Atlas (TCGA)[15] and The Genotype-Tissue Expression (GTEx) public resources.[16] In the GEO database, the keywords "ovarian cancer" and "carcinoma of ovary" were entered to retrieve the transcript data of EOC and nontumor control tissues. Unstandardized mRNA expression values were normalized by $\log_2(x+0.001)$ formula. To obtain the data of the TCGA-GTEx cohort, TCGA and GTEx data in FPKM format were downloaded through the UCSC Xena database,[17] and mRNA expression values from the two datasets were normalized by $\log_2(x+0.001)$ formula and converted into the TPM format; then, the expression information of normal ovarian tissues was extracted from GTEx data and integrated into the mRNA expression matrix of EOC tissues from TCGA. R package impute (http://bioconductor.org/packages/impute/) was used to process missing values in all mRNA expression matrix. The clinical data of patients with EOC were also downloaded from the UCSC Xena platform.

Analysis of the Protein Expression Level of PDZD11 in EOC

After obtaining informed written consent from each patient, we collected 37 cases of normal ovarian tissues, 38 cases of primary EOC samples, and 40 cases of metastatic EOC specimens (Table 1) from Guangxi Medical University Cancer Hospital from January 2023 to November 2023. Normal ovarian tissues were obtained from non-malignant cases, and all were pathologically diagnosed as non-diseased ovarian tissues. All EOC tissues were pathologically diagnosed as serous histological type. The research was conducted in accordance with the Declaration of Helsinki, and approved by the Medical Ethics Committee of Guangxi Medical University Cancer Hospital (protocol code: LW2023003, January 5, 2023). After being deparaffinized, rehydrated and repaired, tissue sections were incubated with the primary antibody against *PDZD11* (1/850 dilution, PHW3840, Abmart, Shanghai, China), and combined with goat anti-rabbit antibody (MaxVision TM HRP-Polymer anti-Rabbit IHC Kit, MAIXIN BIOTECH, Fuzhou, China). Finally, tissue slices were stained using DAB and counterstained with hematoxylin. The staining intensity (SI) and the proportion of positive cells (PP) were evaluated by two pathologists in 10 randomly selected fields under a microscope. Immunoreactive score (IRS) = SI × PP. SI was assigned as: 0 = negative, 1 = weak, 2 = moderate, or 3 = strong. PP was defined as 0 = 0%, 1 = 0–10%, 2 = 11–50%, 3 = 51–80%, and 4 = 81–100%.

Diagnostic Value Analysis of PDZD11 in EOC

Receiver operating characteristic (ROC) curves were plotted using GraphPad Prism 9 software, and the area under the curve (AUC) was calculated to estimate the discrimination capacity of *PDZD11* for EOC. To achieve higher quality of diagnostic evaluation, the diagnostic information of *PDZD11* from independent ROC curves was integrated into the summary ROC (SROC) curve using Stata 15 software (https://stata.com/).

Prognostic Potential Analysis of PDZD11 in EOC Patients

The ovarian cancer module of Kaplan-Meier (KM) plotter[18] was utilized to examine the correlation between *PDZD11* mRNA levels and EOC patients' survival. Based on the auto select best cutoff value on the website, EOC cases were divided into *PDZD11* high-mRNA level and low-mRNA level groups, and the OS, PFS and PPS of the two groups were compared. The prognostic analysis of *PDZD11* in EOC patients stratified by stage, histology, or therapeutic method was also performed.

GO and KEGG Enrichment

The biological process (BP), cellular component (CC), and molecular function (MF) terms of *PDZD11* were identified by Gene Ontology (GO) analysis, and Kyoto Encyclopedia of Genes and Genomes (KEGG) enrichment was performed to reveal the *PDZD11*-associated pathways. Briefly, based on TCGA-GTEx data, differentially expressed genes (DEGs) in EOC were verified with R package limma (http://bioconductor.org/packages/limma/, thresholds: $|\log_2\text{fold change}| > 1$, adjusted p values < 0.05); *PDZD11* co-expressed genes were screened out through R programming (https://r-project.org/,

Table 1 Relationship Between PDZD11 Expression Levels and Clinicopathologic Variables in EOC Cases Included in This Study

characteristics	TCGA (n = 374)	PDZD11 mRNA expression	p-value	Local primary tissue cases (n = 38)	PDZD11 IRS	p-value	Local metastatic tissue cases (n = 40)	PDZD11 IRS	p-value
		Median (min-max) or mean ± SE			Median (min-max)			Median (min-max)	
Age[a]			0.0078			0.1187			0.0006
≤ Median age	196	5.55 (3.66,6.39)		20	6.00 (1.00,9.00)		21	9.00 (1.00,9.00)	
> Median age	178	5.44 (3.81,6.91)		18	9.00 (2.00,12.00)		19	2.00 (0.00,9.00)	
Grade			0.4229			0.8848			-
G1/G2	43	5.57 (3.73,6.89)		3	9.00 (2.00,9.00)		0	-	
G3	320	5.51 (3.66,6.91)		35	6.00 (1.00,12.00)		40	6.00 (0.00,9.00)	
Missing	11	-							
Stage			0.0133			-			-
I/II	22	5.16 ± 0.78		2	7.50 (6.00,9.00)		2	1.00 (0.00,2.00)	
III	292	5.47 ± 0.49		28	6.00 (1.00,12.00)		22	5.00 (0.00,9.00)	
IV	57	5.52 ± 0.48		8	9.00 (2.00,9.00)		16	6.00 (0.00,9.00)	
Missing	3	-							
Histological types			-			-			-
Serous	374	5.50 (3.66,6.91)		38	6.00 (1.00,12.00)		40	6.00 (0.00,9.00)	
Endometrioid	0	-		0			0		
Mucinous	0	-		0			0		
Lymphatic metastasis			0.9645			0.0288			0.7664
Yes	100	5.50 (4.23,6.89)		21	6.00 (1.00,9.00)		20	6.00 (0.00,9.00)	
No	47	5.46 (3.66,6.68)		17	9.00 (4.00,12.00)		20	6.00 (0.00,9.00)	
Missing	227	-							
Race			0.2364			-			-
White	324	5.51 (3.66,6.91)		0			0		
Black	25	5.42 (3.81,6.84)		0			0		
Asian	11	5.47 (4.79,6.68)		38	6.00 (1.00,12.00)		40	6.00 (0.00,9.00)	
Others	3	5.15 (4.57,5.58)							
Missing	11								

Note: [a]Median age of TCGA cases is 59; of local primary tissues cases is 55; and of local metastatic tissues cases is 53.
Abbreviation: IRS, immunoreactive score.

thresholds: | r | > 0.3 and $p < 0.05$). Eventually, the intersection genes of the DEGs and the *PDZD11* co-expressed genes were brought into GO and KEGG analyses through the R package cluster Profiler (http://bioconductor.org/packages/clusterProfiler/).

Correlation Analysis Between PDZD11 mRNA Levels and Immune Infiltration in EOC

The TIMER database[19] was used to assess the correlations between *PDZD11* expression and the infiltration abundances of six types of infiltrating immune cells in EOC. The infiltration proportions of 22 types immune cell subsets in the 379 EOC samples from TCGA were further calculated by CIBERSORT[20] (https://cibersortx.stanford.edu/) tool. Based on the median expression value of *PDZD11*, the 379 EOC samples were grouped into high-mRNA level and low-mRNA level patient sets, and the infiltration levels of 22 types of immune cells in the two sets were compared. Associations of *PDZD11* mRNA levels and immune checkpoints were assessed using the correlation module of TIMER.

Statistical Analysis

PDZD11 expression in different groups was compared using Student's *t*-test, Mann–Whitney test, one-way ANOVA test, Kruskal–Wallis test, or chi-square test. The standardized mean difference (SMD) of *PDZD11* expression was calculated by the R package Meta (https://github.com/guido-s/meta). Survival analysis of EOC patients was performed using KM analysis and the log rank test. Infiltration fractions of 22 types of immune cells between *PDZD11* high-mRNA level and low-mRNA level patient sets were compared using the Mann–Whitney test. Genes co-expressed with *PDZD11* were screened out based on Pearson' s correlation. Moreover, the correlation analyses between *PDZD11* expression and immune checkpoints were performed using Pearson's correlation or Spearman correlation. Statistical analyses were performed by SPSS23.0 and GraphPad Prism 9 and partially visualized by Sangerbox 3.0 tool.[21] $P < 0.05$ were considered statistically significant.

Results

Transcription Expression of PDZD11 in EOC and Other Cancers

We assessed *PDZD11* mRNA levels in 11 different GEO datasets (Table S1), of which six (GSE10971, GSE119054, GSE14407, GSE15578, GSE27651, and GSE38666) showed that EOC tissues had an enhanced level of *PDZD11* expression compared with normal tissues (Figure 1A–D, F and G), whereas no significant differences in *PDZD11* expression between the two types of tissues were observed in another five GEO datasets (Figure 1E and 1H-K). Additionally, upregulation of *PDZD11* expression in EOC was further confirmed in the TCGA-GTEx ovarian cohort (Figure 1L). Furthermore, the SMD was calculated to comprehensively analyze the expression of *PDZD11*. The random-effect model was selected in this study because the heterogeneity was obvious ($I^2 > 50\%$). SMD > 0 suggested that *PDZD11* was generally upregulated in EOC tissues compared with the control group (Figure 1M).

The Protein Expression Level of PDZD11 in EOC

Upregulated PDZD11 protein expression was observed in 78 EOC cases (38 primary tissues and 40 metastatic tissues) with histological type of serous, compared with 37 normal ovarian samples (Figure 1N). Metastatic EOC tissues had a slightly lower proportion of high PDZD11 protein expression level than primary EOC tissues (Figure 1O).

PDZD11 Expression in EOC Patients with Different Clinicopathological Characteristics

We analyzed the correlations between *PDZD11* expression and clinicopathological parameters of EOC patients, based on clinical information of 374 EOC patients from the TCGA open resource and 78 local EOC cases. Our results suggested that *PDZD11* mRNA expression was remarkably elevated in EOC patients with advanced cancer stages (Table 1). Interestingly, in the 38 cases of primary EOC tissues collected in this study, the PDZD11 protein was downregulated in

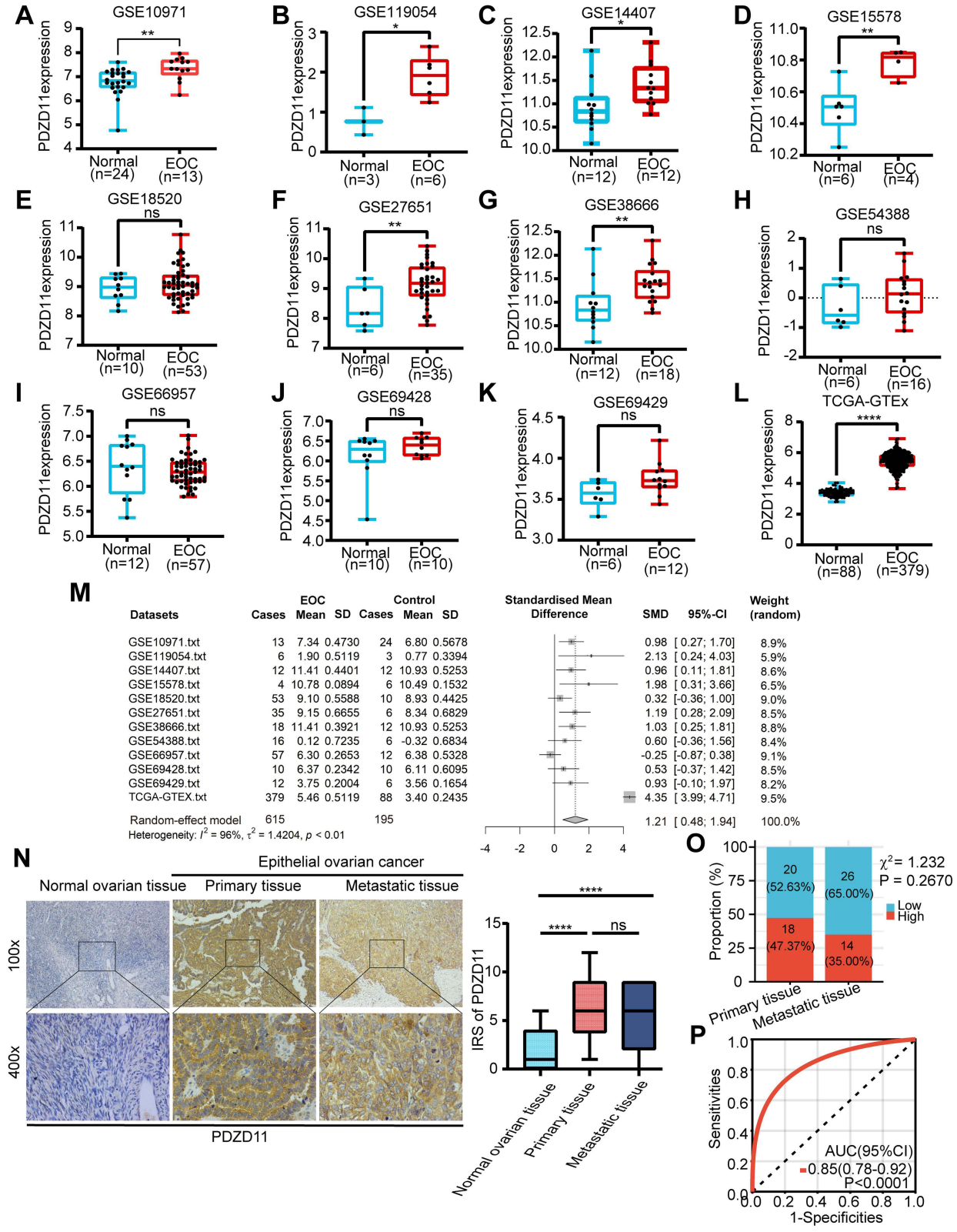

Figure 1 Expression levels of *PDZD11* in epithelial ovarian cancer (EOC). (**A-K**) Comparison of *PDZD11* transcriptional expression levels between EOC tissues and normal controls in 11 different GEO datasets. (**L**) *PDZD11* was overexpressed in EOC tissues in the TCGA-GTEx cohort. (**M**) Standardized mean difference of *PDZD11* expression level base on all datasets included in this study. (**N**) IHC result of *PDZD11* expression in noncancerous ovarian tissues (n = 37), primary EOC tissues (n = 38), and metastatic EOC tissues (n = 40). (**O**) Distribution ratio of PDZD11 protein expression level in primary EOC tissues and metastatic EOC tissues. (**P**) The ability of PDZD11 protein to distinguish cancerous from non-cancerous tissues analyzed in local 78 EOC tissues and 37 normal ovarian samples. -/ns, $P > 0.05$; *, $P < 0.05$; **, $P < 0.01$; ****, $P < 0.0001$.

EOC patients with lymph node metastasis (Table 1). Moreover, in local metastatic tissue cases, PDZD11 level was strongly related to younger age (Table 1).

Diagnostic Value of PDZD11 in EOC

ROC curves and a SROC curve were drawn to assess the ability of *PDZD11* to distinguish EOC from normal tissues. According to AUC, moderate diagnostic accuracy (AUC = 0.85 and $p < 0.0001$) of PDZD11 protein was observed in local EOC cases (Figure 1P); high diagnostic accuracy (AUC > 0.9 and $p < 0.05$) of *PDZD11* mRNA was observed in data sets GSE119054 (Figure 2B), GSE15578 (Figure 2D), and TCGA-GTEx (Figure 2L); moderate diagnostic accuracy

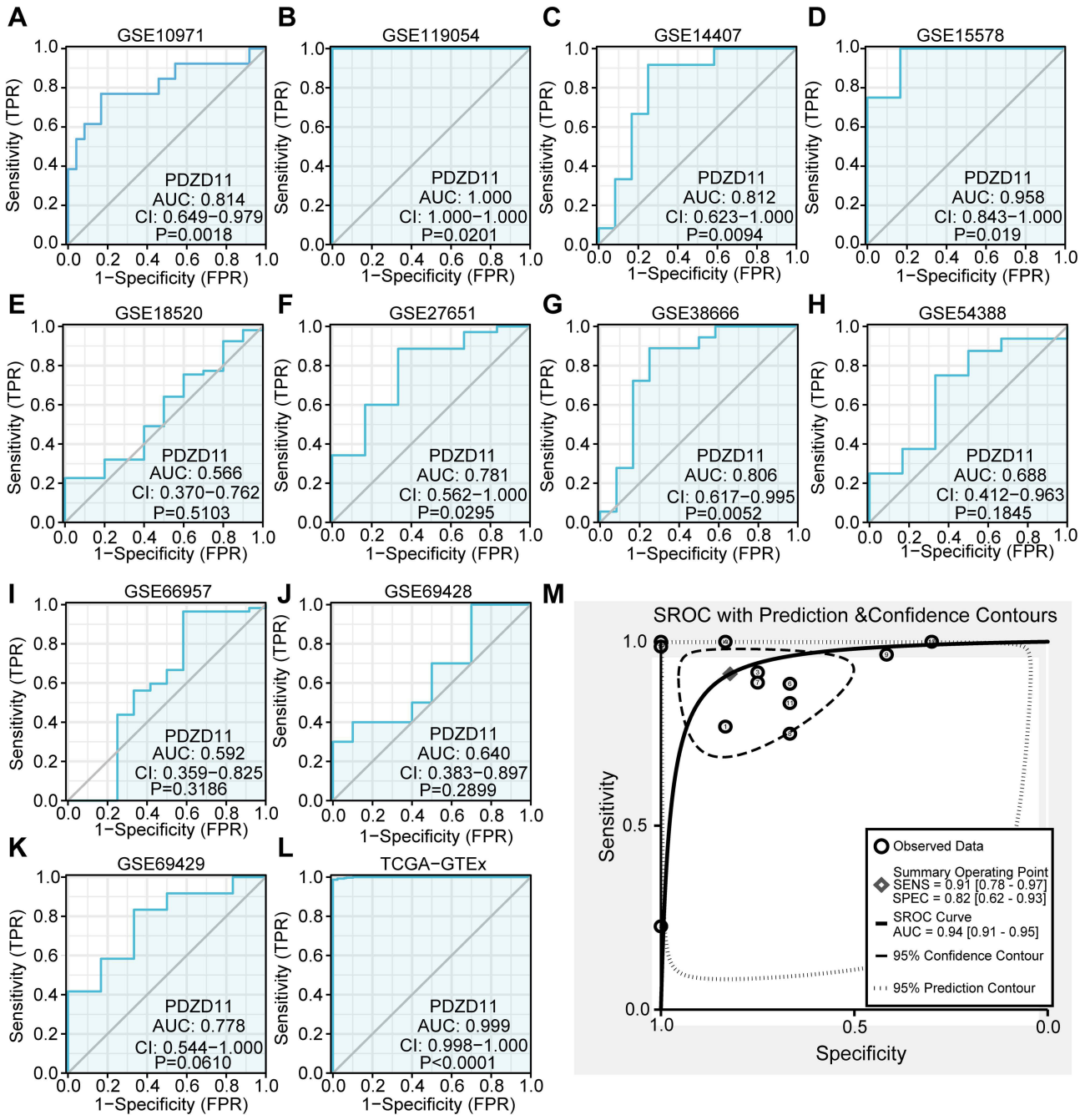

Figure 2 Diagnostic performance of *PDZD11* mRNA levels in EOC based on GEO, TCGA, and GTEx data. (**A-L**) Sensitivity and specificity of *PDZD11* in the 12 patient sets are shown by receiver operating characteristic (ROC) curves. (**M**) The summary ROC curve integrated information from the 12 independent ROC curves, showing the comprehensive diagnostic value of *PDZD11* in EOC.

(AUC = 0.7–0.9 and $p < 0.05$) of *PDZD11* mRNA was observed in data sets GSE10971 (Figure 2A), GSE14407 (Figure 2C), GSE27651 (Figure 2F), and GSE38666 (Figure 2G), while *PDZD11* mRNA showed poor diagnostic accuracy (AUC = 0.5–0.7 or $p > 0.05$) in datasets GSE18520 (Figure 2E), GSE54388 (Figure 2H), GSE66957 (Figure 2I), GSE69428 (Figure 2J), and GSE69429 (Figure 2K), respectively. More importantly, the SROC curve indicated that *PDZD11* mRNA has high comprehensive diagnostic accuracy with AUC = 0.94 ($p < 0.0001$) in EOC (Figure 2M).

Prognostic Value of PDZD11 in EOC Patients

To determine the prognostic potential of *PDZD11*, the correlation between *PDZD11* mRNA levels and the outcomes of EOC patients was investigated using the KM plotter. Elevated *PDZD11* expression was related to worse OS and PFS in EOC cases in the KM database (Figure 3A). Also, stratified survival analysis suggested that a higher *PDZD11* mRNA level was markedly linked with inferior OS in EOC patients at advanced cancer stages (stages 3 or 4) or in EOC cases with the cancer histological type of endometrioid carcinoma (Figure 3B and 3C). Furthermore, increased *PDZD11* mRNA level was correlated with poor PFS in EOC cases with advanced cancer stages or in EOC patients with the cancer histological types of serous or endometrioid carcinoma (Figure 3B and 3C). Interestingly, the *PDZD11* expression levels could also predict the prognoses of EOC patients receiving different treatments. Patients with a higher mRNA level of *PDZD11* had worse OS after suboptimal debulk (Figure 3D). Similarly, patients with lower expression of *PDZD11* had better prognosis after chemotherapy containing taxol, platinum, or taxol combined with platinum (Figure 3D).

GO and KEGG Analyses of PDZD11 in EOC

To investigate the role of *PDZD11* in EOC, we identified 930 overexpressed genes that were positively correlated with *PDZD11* and 1,148 downregulated genes that were negatively correlated with *PDZD11* in EOC from TCGA database for GO and KEGG analyses, respectively. The top 60 *PDZD11*-associated genes in EOC are shown in the heatmap (Figure 4A). For genes positively correlated with *PDZD11* expression, the top five BP terms of enrichment were nuclear division, humoral immune response, chromosome segregation, mitotic nuclear division, and immunoglobulin-mediated immune response; the top five CC terms enriched were cell–cell junction, apical plasma membrane, apical junction complex, tight junction, and bicellular tight junction; the top five MF terms enriched were cadherin binding, antigen binding, cell adhesion mediator activity, cell–cell adhesion mediator activity, and virus receptor activity (Figure 4B). KEGG enrichment analysis indicated that *PDZD11* was correlated with cell adhesion molecules and the cell cycle (Figure 4C). Notably, *PDZD11* was also associated with immune responses, such as human papillomavirus infection, Epstein−Barr virus infection, human T-cell leukemia virus 1 infection, Staphylococcus aureus infection, phagosome, pathogenic Escherichia coli infection, leukocyte transendothelial migration, antigen processing and presentation, Th1 and Th2 cell differentiation, intestinal immune network for IgA production, and autoimmune thyroid disease (Figure 4C).

For genes negatively correlated with *PDZD11* expression, the main enriched BP, CC, and MF are shown in the bubble diagram (Figure 4D). KEGG pathways enriched of these genes included the Ras signaling pathway, the Rap1 signaling pathway, choline metabolism in cancer, and platinum drug resistance (Figure 4E). Our results suggest that *PDZD11* may affect cell adhesion, cell proliferation, immune responses, and certain tumor-related signaling pathways.

Association Between PDZD11 mRNA Levels and Immune Infiltration in EOC

Studies have found that tumor-infiltrating immune cells were connected with cancer development and prognoses in EOC patients.[22,23] Interestingly, the enrichment analyses described above revealed that *PDZD11* was associated with immune responses in EOC. Hence, we used the TIMER online tool to assess the associations between *PDZD11* expression and the infiltration proportions of six common types of immune cells in EOC. *PDZD11* displayed positive correlations with the infiltration abundances of neutrophils, macrophages, dendritic cells, CD8+ T cells, and CD4+ T cells (Figure 5A). To further study the associations between *PDZD11* mRNA levels and infiltration abundances of more immune cell subsets, we used the analytical tool CIBERSORT to compute the infiltrating proportions of 22 types of immune cells in 379 EOC samples from the TCGA database. High infiltrating proportions of T cells and macrophages in EOC were observed in the heat map (Figure 5C). Subsequently, infiltration levels of the 22 types of immune cells in the *PDZD11* high-mRNA level

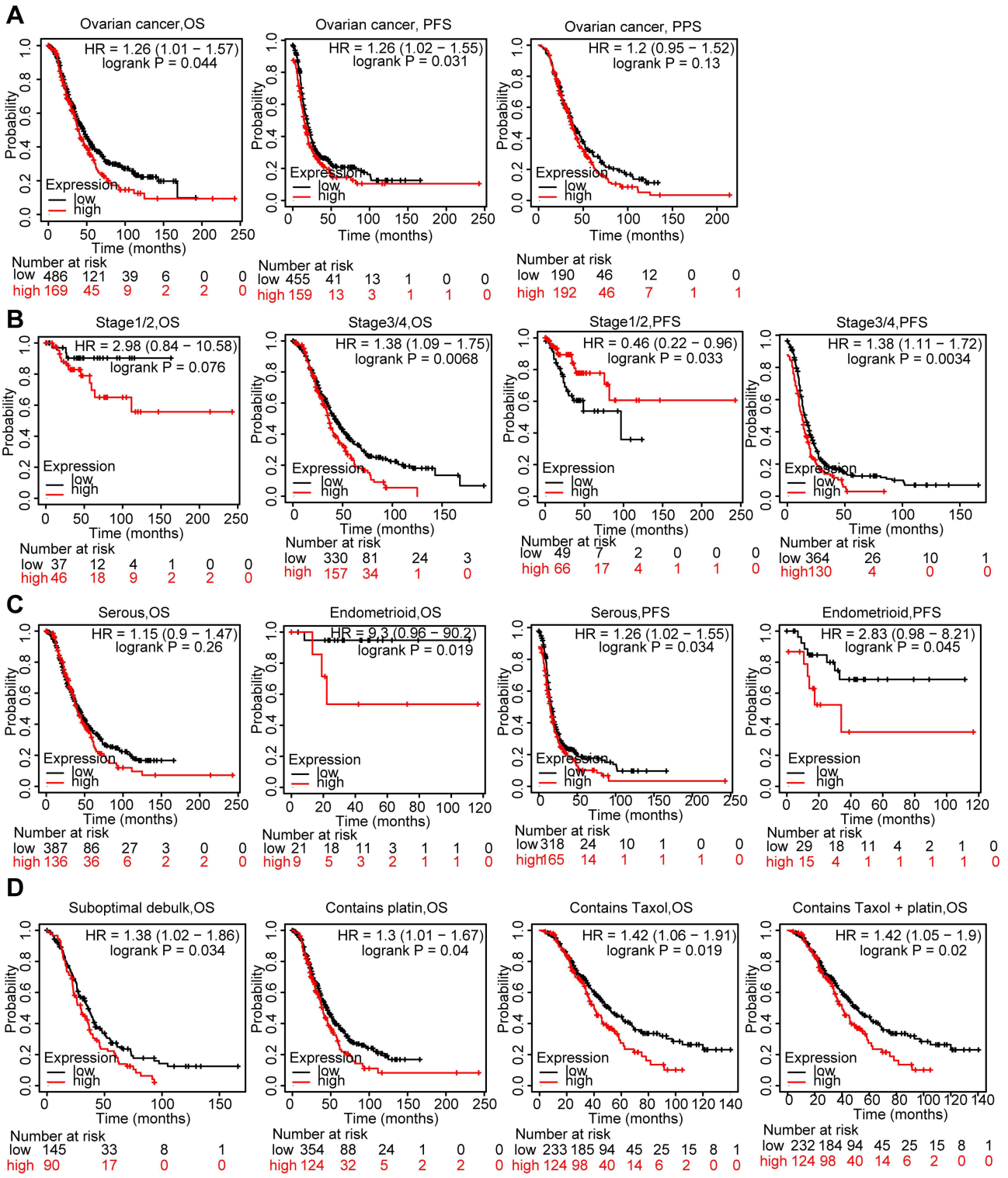

Figure 3 Prognostic potential of *PDZD11* in EOC analyzed in the Kaplan-Meier (KM) plotter. (**A**) KM estimates of OS, PFS, and PPS in EOC patients with different *PDZD11* mRNA levels. Prognostic value analysis of *PDZD11* stratified by (**B**) cancer stages, (**C**) histological types, and (**D**) therapeutic methods.
Abbreviations: HR, hazard ratio; CI, confidence interval.

and low-mRNA level samples were compared. The infiltration levels of CD8+ T cells, follicular helper T cells, Gamma Delta T cells, and M1 macrophages in the *PDZD11* high-expression samples were elevated compared with the low-expression samples, while resting natural killer cells and M0 macrophages were the opposite (Figure 5B). However, no obvious differences were found in the infiltration fractions of other immune cells between the two groups (Figure 5B).

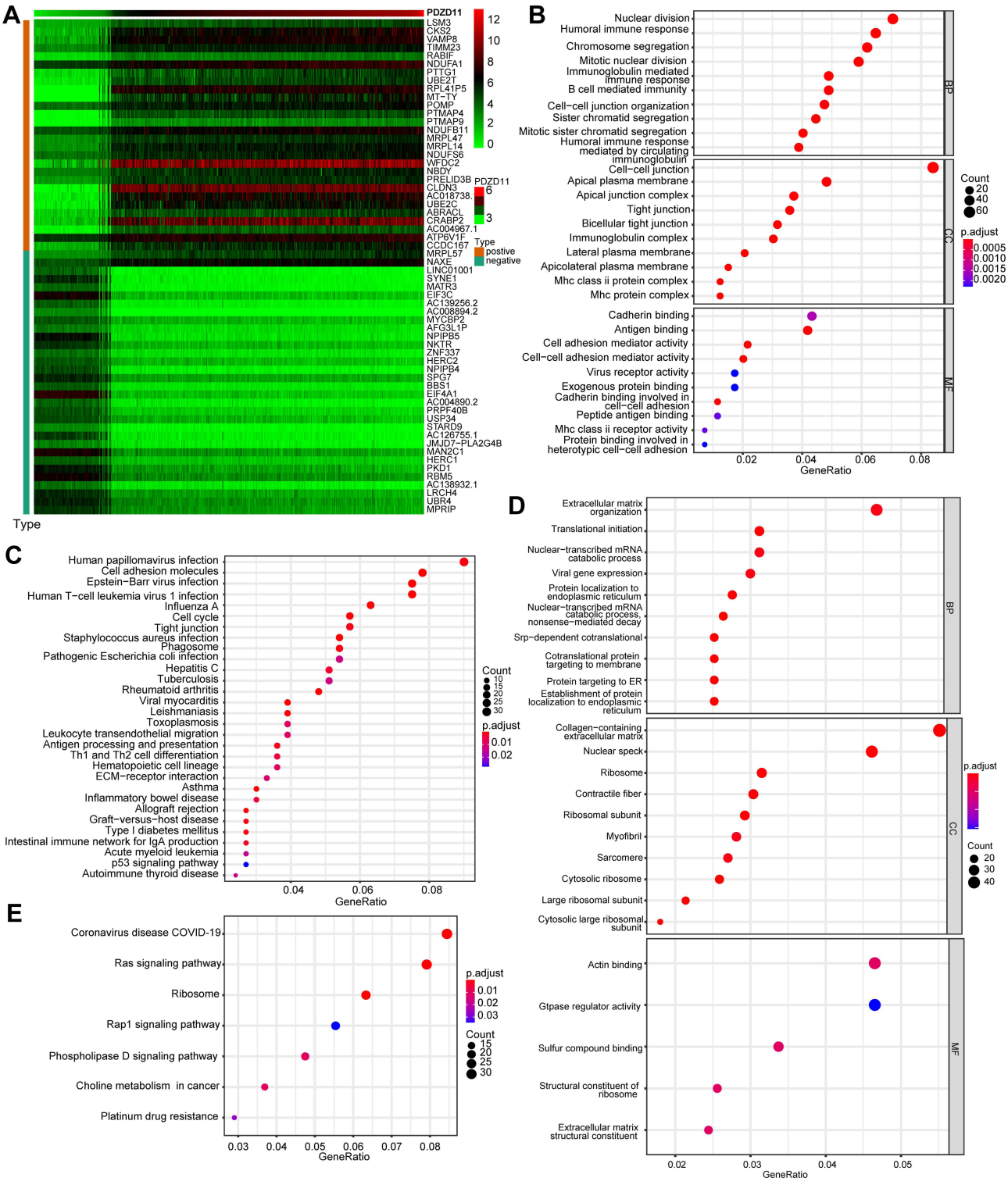

Figure 4 Gene Ontology (GO) and Kyoto Encyclopedia of Genes and Genomes (KEGG) enrichment analyses for *PDZD11* and its co-expressed genes in EOC. (**A**) Heatmap showing the top 60 *PDZD11* co-expressed genes in EOC in the TCGA data. Bubble chart exhibiting the top 10 terms of the biological process (BP), cellular component (CC), and molecular function (MF) enriched of *PDZD11* (**B**) positively and (**D**) negatively co-expressed genes in EOC, respectively. (**C**) Bubble chart showing the top 30 signaling pathways enriched of *PDZD11* positively co-expressed genes in EOC. (**E**) Bubble chart showing the top seven signaling pathways of enrichment of *PDZD11* negatively co-expressed genes in EOC.

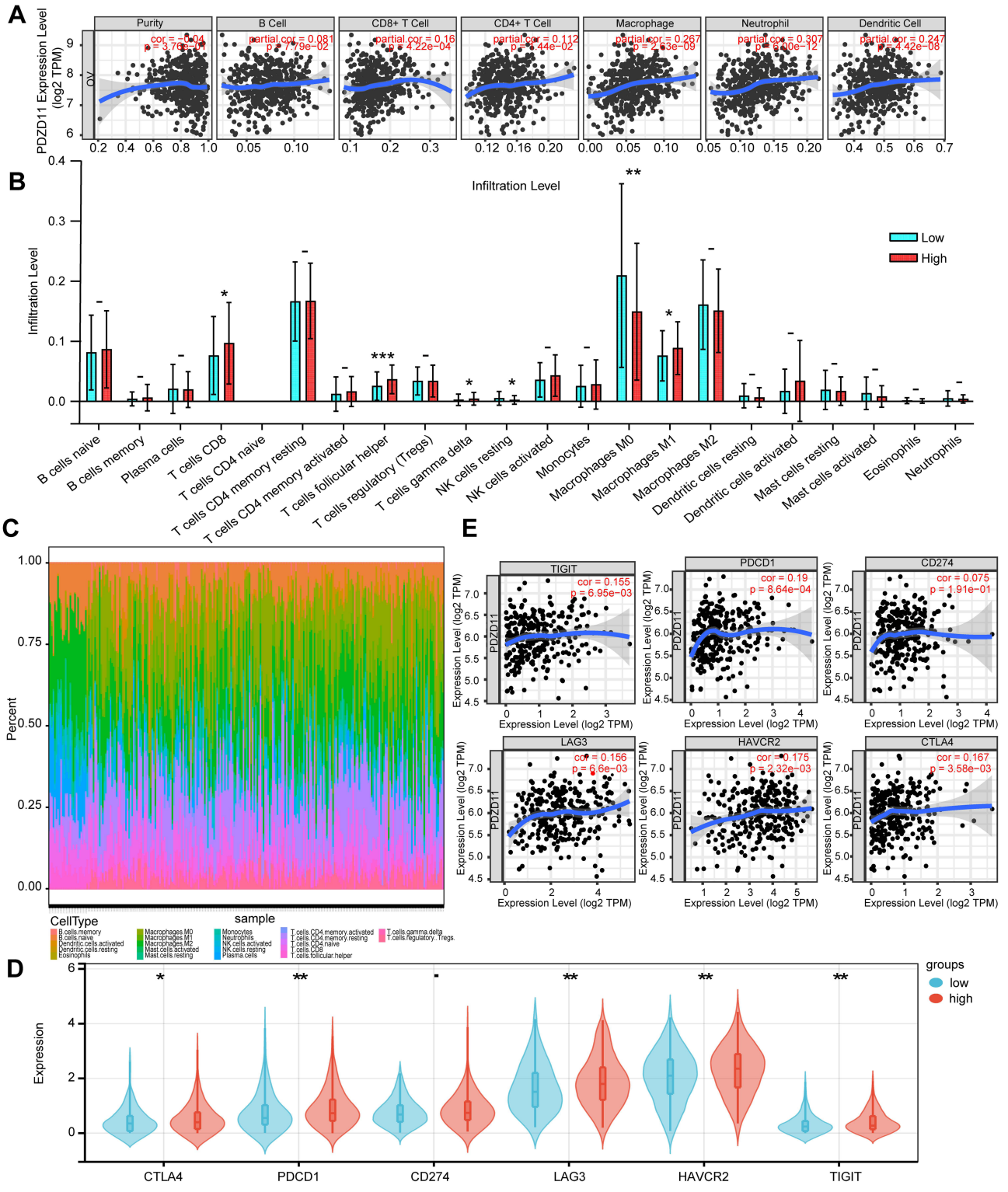

Figure 5 Immune landscape of *PDZD11* in EOC analyzed in TIMER and TCGA database. (**A**) Associations between *PDZD11* expression and infiltration proportions of six common types of immune cells in EOC in TIMER. (**B**) Comparisons of the infiltration levels of diverse immune cells in *PDZD11* high-mRNA level and low-mRNA level EOC samples from the TCGA database. (**C**) Infiltration proportions of the 22 types of immune cells in EOC in TCGA, calculated by the CIBERSORT algorithm. (**D**) The expression of immune checkpoints in the *PDZD11* high-mRNA level group compared with the low-mRNA level group based on TCGA data. (**E**) Expression correlations between *PDZD11* and immune checkpoints in EOC analyzed in TIMER. -, $P > 0.05$; *, $P < 0.05$; **, $P < 0.01$; ***, $P < 0.001$.

https://doi.org/10.2147/IJGM.S459418 DovePress

Correlations Between PDZD11 and Expression of Immune Checkpoints

Immune checkpoint blockade (ICB) therapy is one of the methods of immunotherapy against tumors and have been approved for the treatment of melanoma,[24] lung cancer,[25] renal cell carcinoma[26] and other cancers. Although immune checkpoint inhibitors alone are ineffective for EOC patients, they have been shown to be effective in combination with chemotherapy, targeted therapy, and PARP inhibitors.[27,28] It is shown that PARP inhibitors may enhance the efficacy of immune checkpoint inhibitors (ICIs) through multiple potential immune-enhancing mechanisms. Tumors with homologous recombination deficiency have higher mutation, which enhances neoantigen formation, increasing stronger immune response against cancer.[29] Also, evidence has indicated that PARP inhibitors facilitate interferon type I response by activating the cyclic GMP-AMP synthase-STING pathway, enhancing antigen presentation.[30] Moreover, PARP inhibitors have been shown to upregulate PD-L1 expression by inactivating glycogen synthase kinase 3β, weakening tumor immune response,[29] and this could be rescued by PD-L1 blockade.[29] We thus performed the correlation analyses between *PDZD11* mRNA levels and well-known immune checkpoints, including TIGIT, HAVCR2 (TIM3), LAG3, CTLA4, PDCD-1 (PD-1), and CD274(PD-L1). The expressions of TIGIT, TIM3, LAG3, CTLA4, and PD-1 in the *PDZD11* high-expression samples were higher than in the *PDZD11* low-expression samples based on TCGA data, while *PDZD11* was not significantly correlated with PD-L1 expression levels (Figure 5D). We also calculated the correlation coefficients between *PDZD11* expression and the above six immune checkpoints in EOC using the correlation module of TIMER. *PDZD11* was positively correlated with TIGIT, TIM3, LAG3, CTLA4, and PD-1, but not with PD-L1 (Figure 5E).

Discussion

Growing studies have found that *PDZD11* is a gene related to AJs.[8–11,31,32] However, the potential effect of its abnormal expression on tumorigenesis has rarely been investigated. Our comprehensive analysis indicated that *PDZD11* expression was strongly increased in EOC tissues compared with control samples (Figure 1). *PDZD11* were closely related to cancer stages and no lymph node metastasis status (Table 1), which demonstrated that *PDZD11* may be associated with tumor development of EOC. Subsequently, the ROC and SROC curves showed that *PDZD11* had a certain ability to distinguish EOC tissues from normal tissues (Figure 1P and 2). The KM plotter results demonstrated that the *PDZD11* expression levels could predict the survival of EOC patients. EOC patients with increased *PDZD11* expression had short OS and PFS time (Figure 3A). Also, for EOC patients at advanced cancer stages or with the cancer histological type of endometrioid carcinoma, elevated *PDZD11* expression was significantly linked with poor OS (Figure 3B and 3C). Furthermore, for EOC patients at advanced cancer stages or with the histological types of serous or endometrioid carcinoma, higher *PDZD11* expression was correlated with worse PFS (Figure 3B and 3C). A similar prognostic significance of *PDZD11* was observed in EOC patients receiving different treatments. Patients with lower *PDZD11* mRNA expression level have a better prognosis after suboptimal debulk or chemotherapy containing taxol, platinum, or taxol combined with platinum (Figure 3D). Although this work discovered that *PDZD11* expression was elevated in EOC and exhibited certain diagnostic and prognostic potential, the clinical availability of these results needs to be validated in multi-level, multi-sample, and multi-center studies. More importantly, the difference in serum *PDZD11* expression levels between EOC patients and healthy individuals also remains to be validated to test whether it is convenient for clinical detection.

EOC remains refractory due to its characteristics of extensive pelvic and abdominal metastases. Studies have reported that EMT is a crucial process in cancer metastasis.[33,34] Epithelial cancer cells lose their typical cell–cell junctions, as well as apical-basal polarity, and gain some characteristics of mesenchymal cells to facilitate migration and to achieve the invasion-metastasis cascade.[35] Our results of GO analysis indicated that *PDZD11*-co-expressed genes were mainly enriched in BP terms of cell–cell junction organization and in CC terms of cell–cell junction, apical junction complex, tight junction, and bicellular tight junction and involved in cell–cell adhesion-related MFs such as cadherin binding, cell adhesion mediator activity, and cell–cell adhesion mediator activity (Figure 4B). Moreover, *PDZD11* was shown to be involved in the KEGG pathways of cell adhesion molecules and tight junctions (Figure 4C). More importantly, our IHC validation results suggested that metastatic EOC tissues had a slightly higher ratio of low PDZD11 protein expression

levels than primary EOC tissues (Figure 1O), and the PDZD11 protein was downregulated in EOC cases with lymph node metastasis (Table 1). Based on the results above, we speculate that, like other AJ-related proteins, such as E-cadherin, the loss of *PDZD11* may induce EMT. However, in this study, *PDZD11* expression was elevated in EOC tissues, and GO and KEGG analysis indicated that it was associated with nuclear division, chromosome segregation, mitotic nuclear division, and the cell cycle pathway, which illustrated that *PDZD11* may promote the cell proliferation of EOC (Figure 4C). *PDZD11*, like E-cadherin,[36,37] may have a dual role in EOC. It may contribute to the survival and proliferation of cancer cells, and its decreased expression may also promote metastasis.

Recruited by tumor microenvironment (TME), infiltrating immune cells participate in tumor-associated immune responses or tumor escape. Growing research have found that immune cells in TME, including CD8+ cytotoxic T lymphocytes, CD4+ T cells, natural killer cells, dendritic cells, macrophages, B cells, mast cells, and neutrophils, show certain prognostic significance in human cancer.[38] Among them, TAMs,[39] regulatory T cells,[40] and neutrophils[38] play a crucial role in the tumor antigen presentation process blocking and immune surveillance evasion, thereby promoting tumor development, while dendritic cells[41] and CD8+ cytotoxic T lymphocytes[42] play a significant role in killing cancer cells. Effects of infiltrating immune cells on patients' outcomes have been reported in EOC: in patients with high-grade serous EOC, a higher infiltration of CD208+ dendritic cells was found to be associated with better OS,[43] Whereas high level of TAMs correlated with adverse prognosis in EOC.[44] Interestingly, KEGG analysis in this research revealed that *PDZD11* was associated with human papillomavirus infection, human T-cell leukemia virus 1 infection, Staphylococcus aureus infection, pathogenic Escherichia coli infection, leukocyte transendothelial migration, antigen processing and presentation, Th1 and Th2 cell differentiation, and other immune responses (Figure 4C). Consistently, *PDZD11* mRNA expression was remarkably and positively linked with the infiltration proportions of neutrophils, macrophages, dendritic cells, CD8+ T cells, and CD4+ T cells in EOC (Figure 5A).

Immunotherapy, as a cutting-edge therapy, has been proven to improve the survival of many cancer patients.[45] Immunotherapy mainly includes adoptive T-cell therapy, tumor vaccines, and ICB therapy.[27] The generation of immune checkpoints is a way for the body to establish immune tolerance and prevent autoimmunity, and tumors can stimulate the expression of immune checkpoints to achieve immune evasion. We assessed the correlations between *PDZD11* expression and well-known immune checkpoints in EOC. The expression of TIGIT, TIM3, LAG3, CTLA4, and PD-1 in the *PDZD11* high-mRNA level group was higher than in the *PDZD11* low-mRNA level group (Figure 5D). In addition, *PDZD11* was positively correlated with TIGIT, TIM3, LAG3, CTLA4, and PD-1 (Figure 5E). Our findings suggest that *PDZD11* is a biomarker associated with immune infiltration and expression of immune checkpoints in EOC.

However, our research has some limitations. First of all, our conclusions are mostly based on the results of bioinformatics analysis. Although we have verified the differential expression of PDZD11 protein in local EOC cases (37 cases of normal ovarian tissues, 38 cases of primary EOC samples, and 40 cases of metastatic EOC specimens), and analyzed its correlations with patient clinicopathological parameters, validations from multi-level, multi-sample, and multi-center studies are needed. Secondly, the mechanisms of *PDZD11* in tumor-related immune responses in EOC need to be further explored in experimental studies.

Conclusions

In summary, *PDZD11* was upregulated in EOC tissues and showed certain diagnostic ability in EOC. Increased *PDZD11* expression was related to adverse prognosis of EOC patients. *PDZD11* was related to cell adhesion, decreased in EOC patients with lymphatic metastasis, and involved in the process of cell proliferation. *PDZD11* was significantly linked with immune infiltration in EOC and positively correlated with the expression of immune checkpoints, including TIGIT, TIM3, LAG3, CTLA4, and PD-1, suggesting that it may play a certain role in immune responses in EOC. This study concludes that *PDZD11* is a potential diagnostic and prognostic biomarker of EOC.

Abbreviations

AJ, Adherens junction; AUC, Area under the curve; BP, Biological process; CC, Cellular component; CI, Confidence interval; CJs, Cell-cell junctions; DEGs, Differentially expressed genes; EMT, Epithelial mesenchymal transition; EOC,

Epithelial ovarian cancer; FPKM, Fragments per kilobase of exon model per million reads mapped fragments; GEO, Gene Expression Omnibus; GEPIA, Gene Expression Profiling Interactive Analysis; GO, Gene Ontology; GTEx, The Genotype-Tissue Expression; ICIs, Immune Checkpoint Inhibitors; IHC, Immunohistochemical; IRS, Immunoreactive score; KEGG, Kyoto Encyclopedia of Genes and Genomes; KM plotter, Kaplan-Meier plotter; MF, Molecular function; OS, Overall Survival; PFS, Progression Free Survival; PP, Proportion of positive cells; PPS, Post progression survival; ROC, Receiver operating characteristic; SI, Staining intensity; SMD, Standardized mean difference; sROC, Summary receiver operating characteristic; TAMs, Tumor-associated macrophages; TCGA, The Cancer Genome Atlas; TME, Tumor microenvironment; UCSC, University of California Santa Cruz.

Data Sharing Statement

The data that support the findings of this article are available on request from the corresponding author. Public data included in this study are available at the Gene Expression Omnibus (https://www.ncbi.nlm.nih.gov/geo/), The Cancer Genome Atlas (https://portal.gdc.cancer.gov/), Genotype-Tissue Expression (https://gtexportal.org/home/), The Kaplan-Meier plotter (http://kmplot.com), cBioportal (https://www.cbioportal.org/), TIMER database (https://cistrome.shinyapps.io/timer/), and University of California Santa Cruz Xena database (http://xena.ucsc.edu/).

Ethics Approval and Informed Consent

The study was conducted in accordance with the Declaration of Helsinki, and approved by the Medical Ethics Committee of Guangxi Medical University Cancer Hospital (protocol code: LW2023003, date: January 5, 2023). Informed consent was obtained from all subjects involved in the study.

Acknowledgments

We appreciate all open databases and online analytic tools used in this study as well as financial support for this work. We are grateful to Figdraw (https://www.figdraw.com) for the graphical material (authorization ID: YIOWY27f24) in the graphical abstract.

Author Contributions

All authors made a significant contribution to the work reported, whether that is in the conception, study design, execution, acquisition of data, analysis and interpretation, or in all these areas; took part in drafting, revising or critically reviewing the article; gave final approval of the version to be published; have agreed on the journal to which the article has been submitted; and agree to be accountable for all aspects of the work.

Funding

This work was supported by Key Laboratory of Early Prevention and Treatment for Regional High Frequency Tumor (Guangxi Medical University), Ministry of Education (GKE-zz 202018, GKE-zz 202121), Guangxi medical high-level backbone personnel training "139" Project (No.201414, No.201822), Special Fund of the 17th Guangxi New Century "Ten, Hundred, Thousand" Talent Project (No.2014210), Guangxi Zhuang Autonomous Region Key Clinical Specialty Construction Project (2018-39), and Guangxi Natural Science Foundation (2023GXNSFAA026216, 2023GXNSFBA026101).

Disclosure

The authors declare no conflicts of interest.

References

1. Pavlidis N, Rassy E, Vermorken JB, et al. The outcome of patients with serous papillary peritoneal cancer, fallopian tube cancer, and epithelial ovarian cancer by treatment eras: 27 years data from the SEER registry. *Cancer Epidemiol*. 2021;75:102045. doi:10.1016/j.canep.2021.102045
2. Sung H, Ferlay J, Siegel RL, et al. Global Cancer Statistics 2020: GLOBOCAN estimates of incidence and mortality worldwide for 36 Cancers in 185 countries. *CA Cancer J Clin*. 2021;71(3):209–249. doi:10.3322/caac.21660

3. Lheureux S, Gourley C, Vergote I, Oza AM. Epithelial ovarian cancer. *Lancet*. 2019;393(10177):1240–1253. doi:10.1016/S0140-6736(18)32552-2
4. Shah S, Cheung A, Kutka M, Sheriff M, Boussios S. Epithelial ovarian cancer: providing evidence of predisposition genes. *Int J Environ Res Public Health*. 2022;19(13):8113. doi:10.3390/ijerph19138113
5. Boussios S, Moschetta M, Tatsi K, Tsiouris AK, Pavlidis N. A review on pregnancy complicated by ovarian epithelial and non-epithelial malignant tumors: diagnostic and therapeutic perspectives. *J Adv Res*. 2018;12:1–9. doi:10.1016/j.jare.2018.02.006
6. Ghose A, McCann L, Makker S, et al. Diagnostic biomarkers in ovarian cancer: advances beyond CA125 and HE4. *Ther Adv Med Oncol*. 2024;16:17588359241233225. doi:10.1177/17588359241233225
7. Nabokina SM, Subramanian VS, Said HM. Association of PDZ-containing protein PDZD11 with the human sodium-dependent multivitamin transporter. *Am J Physiol Gastrointest Liver Physiol Apr*. 2011;300(4):G561–7. doi:10.1152/ajpgi.00530.2010
8. Shah J, Guerrera D, Vasileva E, Sluysmans S, Bertels E, Citi S. PLEKHA7: Cytoskeletal adaptor protein at center stage in junctional organization and signaling. *Int J Biochem Cell Biol*. 2016;75:112–116. doi:10.1016/j.biocel.2016.04.001
9. Guerrera D, Shah J, Vasileva E, et al. PLEKHA7 Recruits PDZD11 to Adherens Junctions to Stabilize Nectins. *J Biol Chem*. 2016;291 (21):11016–11029. doi:10.1074/jbc.M115.712935
10. Vasileva E, Sluysmans S, Bochaton-Piallat ML, Citi S. Cell-specific diversity in the expression and organization of cytoplasmic plaque proteins of apical junctions. *Ann N Y Acad Sci*. 2017;1405(1):160–176. doi:10.1111/nyas.13391
11. Rouaud F, Tessaro F, Aimaretti L, Scapozza L, Citi S. Cooperative binding of the tandem WW domains of PLEKHA7 to PDZD11 promotes conformation-dependent interaction with tetraspanin 33. *J Biol Chem*. 2020;295(28):9299–9312. doi:10.1074/jbc.RA120.012987
12. Huxham J, Tabaries S, Siegel PM. Afadin (AF6) in cancer progression: a multidomain scaffold protein with complex and contradictory roles. *Bioessays*. 2021;43(1):e2000221. doi:10.1002/bies.202000221
13. Tabaries S, Siegel PM. The role of claudins in cancer metastasis. *Oncogene*. 2017;36(9):1176–1190. doi:10.1038/onc.2016.289
14. Edgar R, Domrachev M, Lash AE. Gene Expression Omnibus: NCBI gene expression and hybridization array data repository. *Nucleic Acids Res*. 2002;30(1):207–210. doi:10.1093/nar/30.1.207
15. Grossman RL, Heath AP, Ferretti V, et al. Toward a shared vision for cancer genomic data. *N Engl J Med*. 2016;375(12):1109–1112. doi:10.1056/NEJMp1607591
16. Consortium GT, Thomas J, Salvatore M. The Genotype-Tissue Expression (GTEx) project. *Nat Genet*. 2013;45(6):580–585. doi:10.1038/ng.2653
17. Goldman MJ, Craft B, Hastie M, et al. Visualizing and interpreting cancer genomics data via the Xena platform. *Nat Biotechnol*. 2020;38 (6):675–678. doi:10.1038/s41587-020-0546-8
18. Gyorffy B, Lanczky A, Szallasi Z. Implementing an online tool for genome-wide validation of survival-associated biomarkers in ovarian-cancer using microarray data from 1287 patients. *Endocr Relat Cancer Apr*. 2012;19(2):197–208. doi:10.1530/ERC-11-0329
19. Li T, Fan J, Wang B, et al. TIMER: a web server for comprehensive analysis of tumor-infiltrating immune cells. *Cancer Res*. 2017;77(21):e108–e110. doi:10.1158/0008-5472.CAN-17-0307
20. Newman AM, Liu CL, Green MR, et al. Robust enumeration of cell subsets from tissue expression profiles. *Nat Methods*. 2015;12(5):453–457. doi:10.1038/nmeth.3337
21. Shen W, Song Z, Zhong X, et al. Sangerbox: a comprehensive, interaction-friendly clinical bioinformatics analysis platform. Commentary. *iMeta*. 2022;1(3):e36. doi:10.1002/imt2.36
22. Luo X, Xu J, Yu J, Yi P. Shaping immune responses in the tumor microenvironment of ovarian cancer. *Front Immunol*. 2021;12:692360. doi:10.3389/fimmu.2021.692360
23. Ning F, Cole CB, Annunziata CM. Driving immune responses in the ovarian tumor microenvironment. *Front Oncol*. 2020;10:604084. doi:10.3389/fonc.2020.604084
24. Weber JS, D'Angelo SP, Minor D, et al. Nivolumab versus chemotherapy in patients with advanced melanoma who progressed after anti-CTLA-4 treatment (CheckMate 037): a randomised, controlled, open-label, Phase 3 trial. *Lancet Oncol Apr*. 2015;16(4):375–384. doi:10.1016/S1470-2045(15)70076-8
25. Wang L, Ma Q, Yao R, Liu J. Current status and development of anti-PD-1/PD-L1 immunotherapy for lung cancer. *Int Immunopharmacol*. 2020;79:106088. doi:10.1016/j.intimp.2019.106088
26. Rini BI, Plimack ER, Stus V, et al. Pembrolizumab plus Axitinib versus Sunitinib for Advanced Renal-Cell Carcinoma. *N Engl J Med*. 2019;380 (12):1116–1127. doi:10.1056/NEJMoa1816714
27. Swiderska J, Kozlowski M, Kwiatkowski S, Cymbaluk-Ploska A. Immunotherapy of ovarian cancer with particular emphasis on the PD-1/PDL-1 as target points. *Cancers (Basel)*. 2021;13(23):6063. doi:10.3390/cancers13236063
28. Kandalaft LE, Odunsi K, Coukos G. Immunotherapy in Ovarian Cancer: Are We There Yet? *J Clin Oncol*. 2019;37(27):2460–2471. doi:10.1200/JCO.19.00508
29. Musacchio L, Cicala CM, Camarda F, et al. Combining PARP inhibition and immune checkpoint blockade in ovarian cancer patients: a new perspective on the horizon? *ESMO Open*. 2022;7(4):100536. doi:10.1016/j.esmoop.2022.100536
30. Mahadevia H, Ponvilawan B, Al-Obaidi A, Buckley J, Subramanian J, Bansal D. Exceptional synergistic response of PARP inhibitor and immune checkpoint inhibitor in esophageal adenocarcinoma with a germline BRCA2 mutation: a case report. *Ther Adv Med Oncol*. 2024;16:17588359241242406. doi:10.1177/17588359241242406
31. Shah J, Rouaud F, Guerrera D, et al. A dock-and-lock mechanism clusters ADAM10 at cell-cell junctions to promote alpha-Toxin cytotoxicity. *Cell Rep*. 2018;25(8):2132–2147 e7. doi:10.1016/j.celrep.2018.10.088
32. Sluysmans S, Mean I, Jond L, Citi S. WW. PH and C-Terminal domains cooperate to direct the subcellular localizations of PLEKHA5, PLEKHA6 and PLEKHA7. *Front Cell Dev Biol*. 2021;9:729444. doi:10.3389/fcell.2021.729444
33. Zhang Y, Weinberg RA. Epithelial-to-mesenchymal transition in cancer: complexity and opportunities. *Front Med*. 2018;12(4):361–373. doi:10.1007/s11684-018-0656-6
34. Brabletz T, Kalluri R, Nieto MA, Weinberg RA. EMT in cancer. *Nat Rev Cancer*. 2018;18(2):128–134. doi:10.1038/nrc.2017.118
35. Jiang Y, Zhan H. Communication between EMT and PD-L1 signaling: new insights into tumor immune evasion. *Cancer Lett*. 2020;468:72–81. doi:10.1016/j.canlet.2019.10.013
36. Padmanaban V, Krol I, Suhail Y, et al. E-cadherin is required for metastasis in multiple models of breast cancer. *Nature*. 2019;573(7774):439–444. doi:10.1038/s41586-019-1526-3

37. Venhuizen JH, Jacobs FJC, Span PN, Zegers MM. P120 and E-cadherin: double-edged swords in tumor metastasis. *Semin Cancer Biol*. 2020;60:107–120. doi:10.1016/j.semcancer.2019.07.020
38. Bruni D, Angell HK, Galon J. The immune contexture and Immunoscore in cancer prognosis and therapeutic efficacy. *Nat Rev Cancer*. 2020;20(11):662–680. doi:10.1038/s41568-020-0285-7
39. Li X, Liu R, Su X, et al. Harnessing tumor-associated macrophages as aids for cancer immunotherapy. *Mol Cancer*. 2019;18(1):177. doi:10.1186/s12943-019-1102-3
40. Nishikawa H, Koyama S. Mechanisms of regulatory T cell infiltration in tumors: implications for innovative immune precision therapies. *J Immunother Canc*. 2021;9(7). doi:10.1136/jitc-2021-002591
41. Fu C, Jiang A. Dendritic cells and CD8 T Cell immunity in tumor microenvironment. *Front Immunol*. 2018;9:3059. doi:10.3389/fimmu.2018.03059
42. Farhood B, Najafi M, Mortezaee K. CD8(+) cytotoxic T lymphocytes in cancer immunotherapy: a review. *J Cell Physiol*. 2019;234(6):8509–8521. doi:10.1002/jcp.27782
43. Truxova I, Kasikova L, Hensler M, et al. Mature dendritic cells correlate with favorable immune infiltrate and improved prognosis in ovarian carcinoma patients. *J Immunother Cancer*. 2018;6(1):139. doi:10.1186/s40425-018-0446-3
44. Zhang QW, Liu L, Gong CY, et al. Prognostic significance of tumor-associated macrophages in solid tumor: a meta-analysis of the literature. *PLoS One*. 2012;7(12):e50946. doi:10.1371/journal.pone.0050946
45. Yang L, Ning Q, Tang SS. Recent advances and next breakthrough in immunotherapy for cancer treatment. *J Immunol Res*. 2022;2022:8052212. doi:10.1155/2022/8052212